Axion, a brief introduction p.2

杨峤立 Qiaoli Yang
Jinan Univ. (Guangzhou)

2022-07-19

Some useful literature:

Rev.Mod.Phys. 93 (2021) 1, 015004

Phys.Rept. 643 (2016) 1-79

Phys.Rev.D 81 (2010) 123530

Phys.Rev.D 59 (1999) 086004

Phys.Rept. 150 (1987) 1-177

Haloscope: a high-Q resonance cavity pickup of the signal

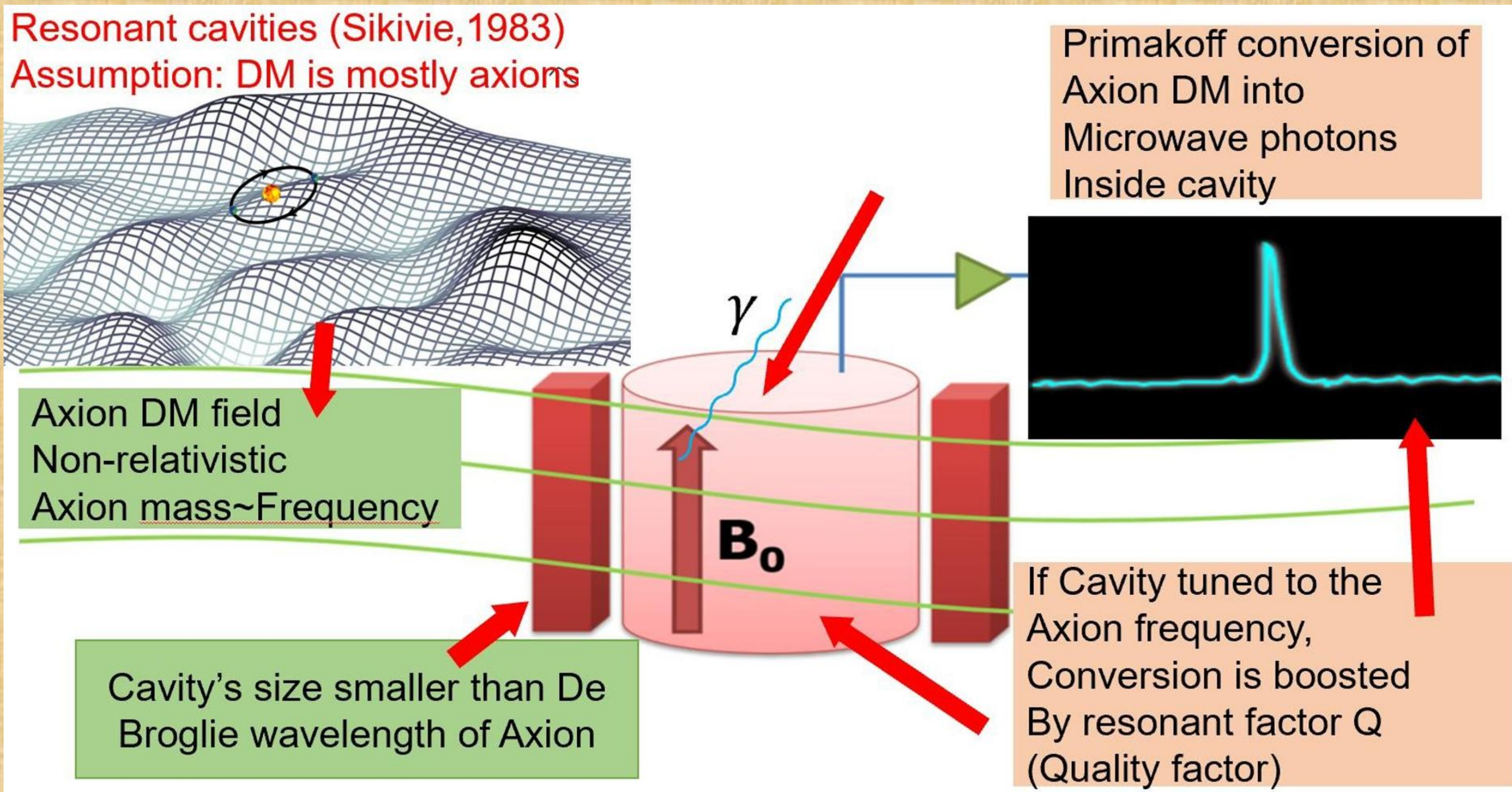

The inverse Primakoff effect:

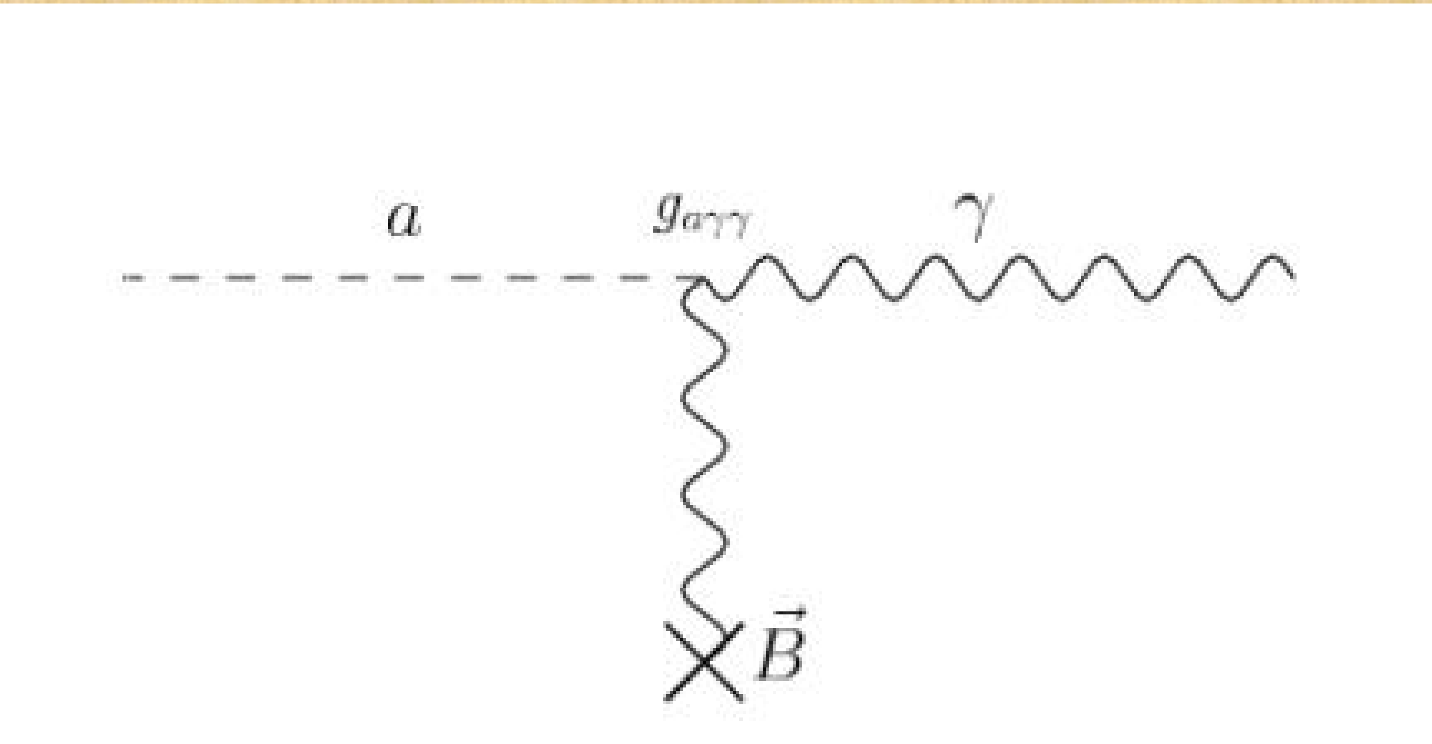

The Sikivie electrodynamics

The Maxwell equations are modified:

$$\mathcal{L}_{a\gamma\gamma} = -\frac{g_{a\gamma}}{4} aF\tilde{F} = -g_{a\gamma}\ a\vec{E}\cdot\vec{B},$$

$$\begin{aligned}
\vec{\nabla}\cdot\vec{E} &= \rho_e + g_{a\gamma}\vec{B}\cdot\nabla a \\
\vec{\nabla}\times\vec{B} - \frac{\partial\vec{E}}{\partial t} &= g_{a\gamma}\vec{E}\times\vec{\nabla}a - g_{a\gamma}\vec{B}\frac{\partial a}{\partial t} + \vec{j}_e \\
\vec{\nabla}\cdot\vec{B} &= 0 \\
\vec{\nabla}\times\vec{E} &= -\frac{\partial\vec{B}}{\partial t}\ ,
\end{aligned}$$

The signal power:

$$\boldsymbol{\nabla} \times \partial_t \mathbf{B} - \partial_t^2 \mathbf{E} = -g_{a\gamma\gamma} B_0 \partial_t^2 a\, \hat{\mathbf{z}}$$

$$\Rightarrow -\boldsymbol{\nabla} \times \boldsymbol{\nabla} \times \mathbf{E} - \partial_t^2 \mathbf{E} = -g_{a\gamma\gamma} B_0 \partial_t^2 a\, \hat{\mathbf{z}}$$

$$-\sum_m \left(\omega_m^2 + \partial_t^2\right) E_m(t)\, \mathbf{e}_m(\mathbf{x}) \cdot \mathbf{e}_n^*(\mathbf{x}) = -g_{a\gamma\gamma} B_0 \partial_t^2 a(t)\, \hat{\mathbf{z}} \cdot \mathbf{e}_n^*(\mathbf{x}).$$

The signal power:

$$\left(\omega_n^2 - \omega^2 - i\frac{\omega\omega_n}{Q_n}\right) E_n(\omega) = g_{a\gamma\gamma} B_0 \frac{\kappa_n}{\lambda_n} \omega^2 a(\omega).$$

$$\begin{aligned}
U_n &= \frac{1}{2} \left\langle E_n^2(t) \right\rangle \int \mathrm{d}^3\mathbf{x} \left[|\mathbf{e}_n(\mathbf{x})|^2 + |\mathbf{b}_n(\mathbf{x})|^2 \right] \\
&= \lambda_n \int_{-\infty}^{\infty} \frac{\mathrm{d}\omega}{2\pi} \left| E_n(\omega) \right|^2 \\
&= g_{a\gamma\gamma}^2 B_0^2 \frac{\kappa_n^2}{\lambda_n} \int_{-\infty}^{\infty} \frac{\mathrm{d}\omega}{2\pi} \frac{\omega^4 \left| a(\omega) \right|^2}{\left(\omega_n^2 - \omega^2\right)^2 + \omega^2 \omega_n^2 / Q_n^2}.
\end{aligned}$$

The signal power:

$$C_{mn\ell} = \frac{\kappa_{mn\ell}^2}{V\lambda_{mn\ell}} = \frac{\left(\int \mathrm{d}^3\mathbf{x}\,\hat{\mathbf{z}}\cdot\mathbf{e}^*_{mn\ell}(\mathbf{x})\right)^2}{V\int \mathrm{d}^3\mathbf{x}\,\varepsilon(\mathbf{x})\,\left|\mathbf{e}_{mn\ell}(\mathbf{x})\right|^2},$$

$$P_{\mathrm{sig}} = \left(g_\gamma^2 \frac{\alpha^2}{\pi^2}\frac{\hbar^3 c^3 \rho_a}{\chi}\right)\left(\frac{\beta}{1+\beta}\omega_c \frac{1}{\mu_0} B_0^2 V C_{mn\ell} Q_L \frac{1}{1+(2\delta\nu_a/\Delta\nu_c)^2}\right),$$

Detect Axion Dark Matter: Haloscope

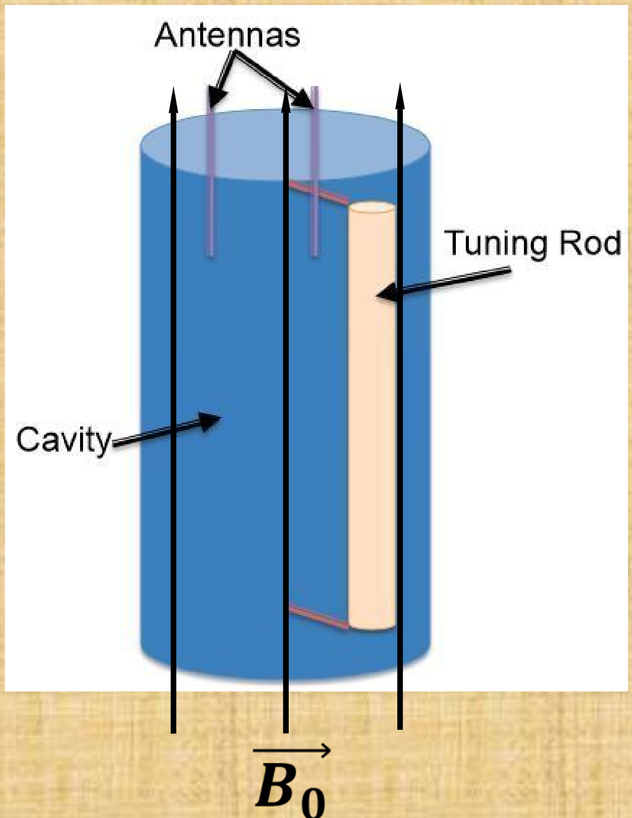

$$P_{signal} = \frac{Q\beta}{(1+\beta)^2} g_{a\gamma\gamma}^2 \left(\frac{\rho_a}{m_a}\right) B_0^2 V C_{010}$$

- Halo axions convert into EM excitation of TM modes of the cavity.
- Equilibrium between axion-stimulated excitation of the mode and spontaneous de-excitation due to thermal relaxation.
- Equilibrium population controlled by axion conversion rate, cavity's quality factor Q
- Power transfer increased by coherence between cavity E-field and axion field

Tunable resonance frequency:
cavity inside a low temperature chamber

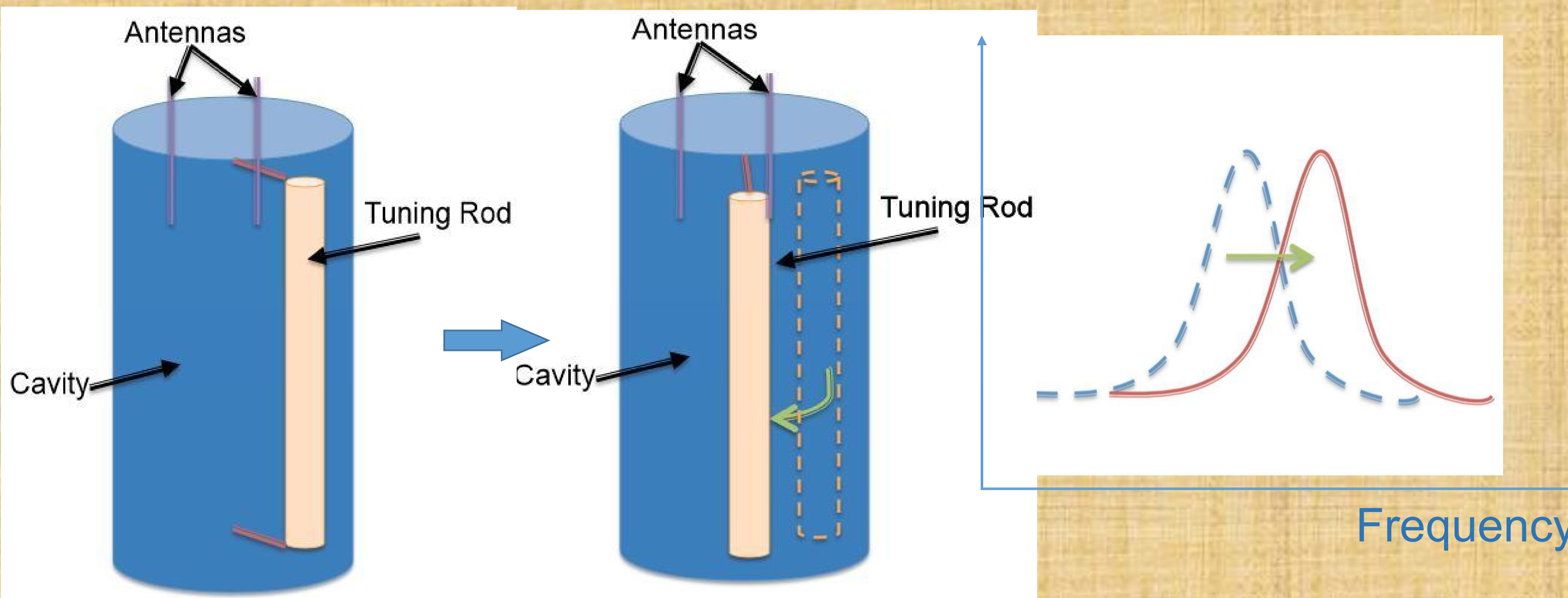

Resonant Cavity Haloscope Structure

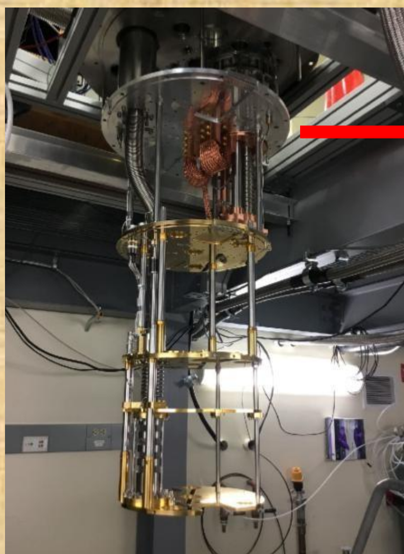

Dilution fridge

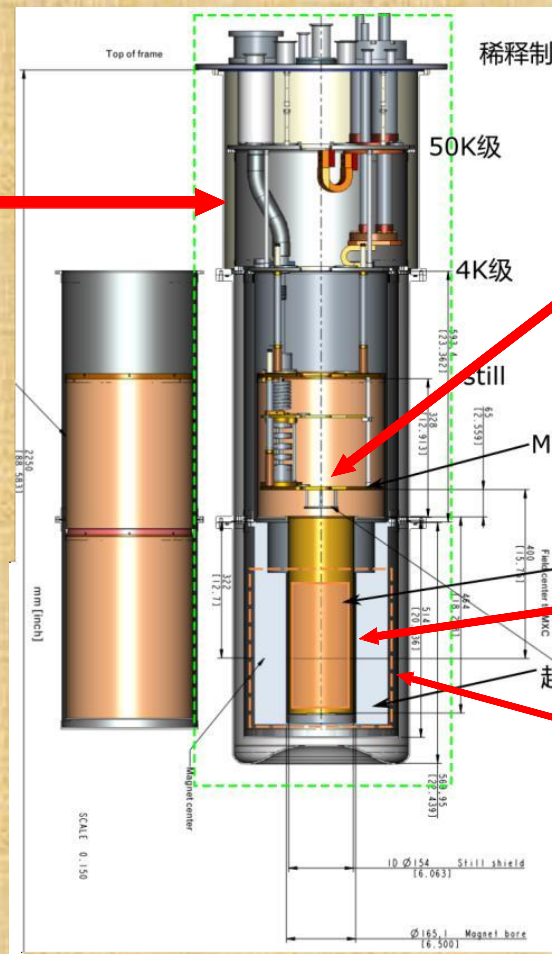

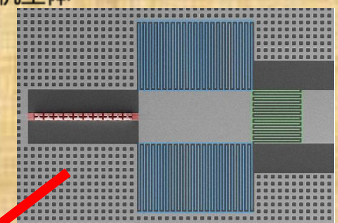

Amplifier (JPA or TWPA)+ Readout

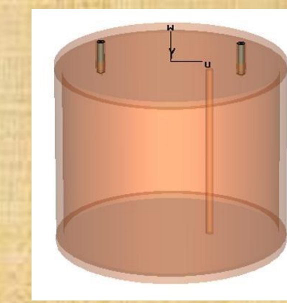

Microwave Cavity
(+ freq. tuning structure)

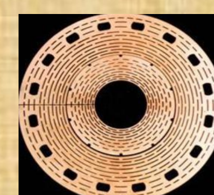

Superconducting solenoid

ADMX (**A**xion **D**ark **M**atter e**X**periment)

Florida(1995-2012)
→
Washington(2012+, Gen2)

ADMX - High Freq
"Sidecar" R&D for 4+GHz.
Now running for
5-7 GHz scan.

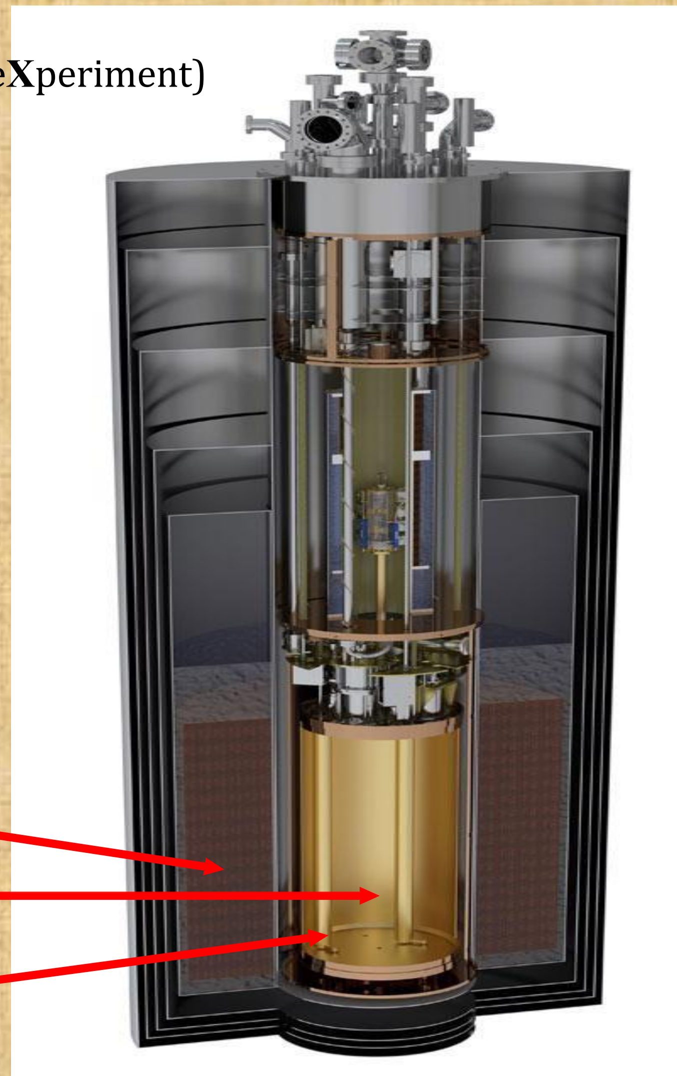

9T Magnet

Microwave Cavity

Tuning Rods

ADMX G2, next steps
Multicavity Systems

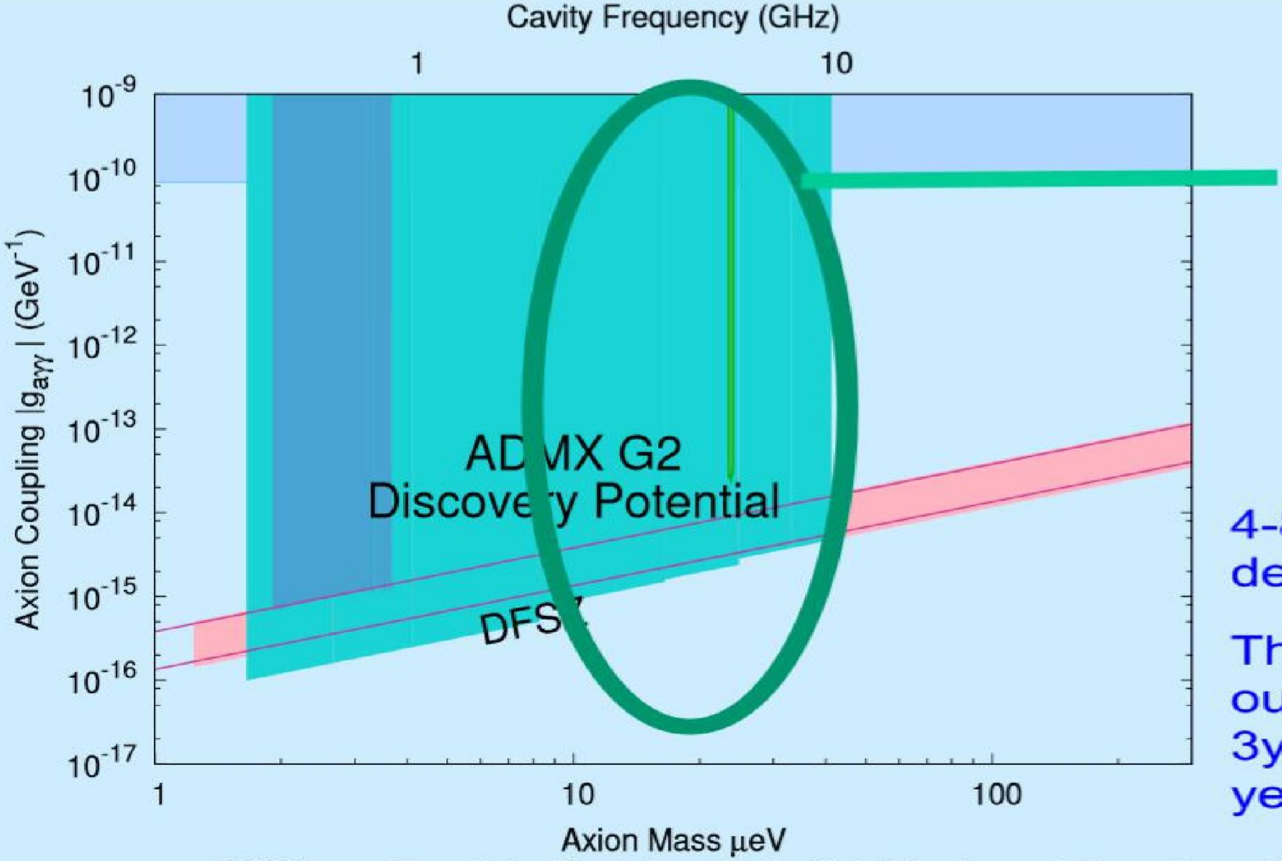

4-8 GHz resonators in design.

This would be beyond our currently approved 3yr funding. Goals for years 3-6.

W. Wester, Fermilab, Workshop on Particle Physics and Cosmology, Zurich Aug 2018

HAYSTAC
(Haloscope at Yale Sensitive to Axion CDM)

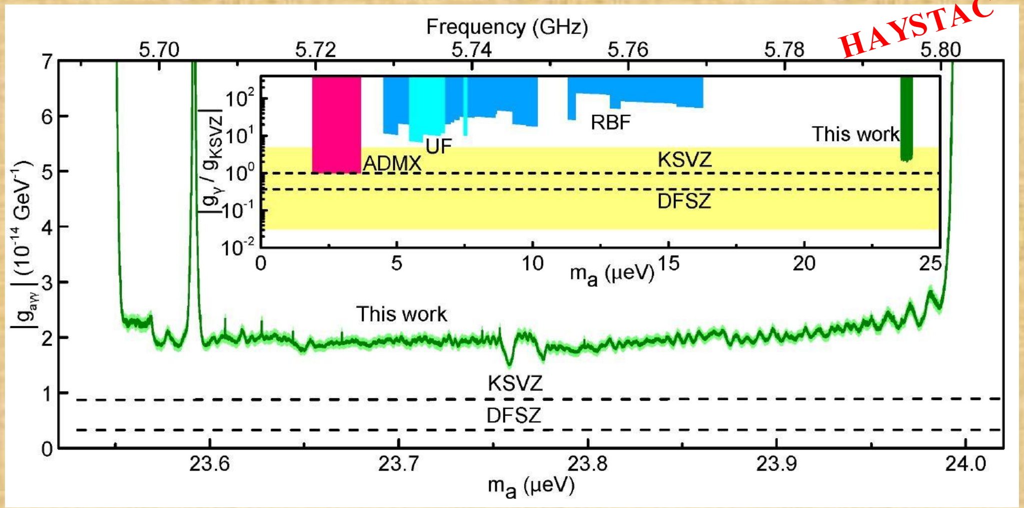

Benjamin M. Brubaker, HAYSTAC first results, 2018

$23.55 < ma < 24.16\mu eV$

Resonance Cavity highlights

Narrow-band detection: high-Q, good bkg veto, supreme sensitivity

Signal from inside:
EM 1~10GHz signal: Low requirement on experimental location

Affordable techniques:
Relatively lower cost: Compared to other fundamental particle searches

Scale-able experiment

Experimental Design

Components	Parameters
Superconducting Magnet	Field strength: 14T Bore: 50mm Height: 20-30cm
Resonant Cavity: Design frequency: 8-10GHz (Corresponding m_a:33-41μeV)	V=0.18L Q~10^5 TM_{010} (C_{010}=0.69) (Test run at 8 GHz)
Cryogenics System	Physical Temperature: 10mK~100mK below electronic noise
Receiver System (include amplifiers, etc.)	Noise temperature: Combining thermal and electronic noises, the target temperature is about 0.5K

Operation at 8 GHz:

- Signal Power: $\mathrm{P_{singal}} \approx 10^{-23}W$
- Scan Rate:

$\frac{df}{dt} \sim 254.24 MHz/year$(KSVZ) $= 4.68 MHz/year$(DFSZ)

- At ν =8 GHz:
- $\frac{S}{N} = \frac{P_{signal}}{k_B T_s}\sqrt{\frac{\delta t}{\delta \nu_a}}$ ~ 3, Signal Band: $\delta\nu_a$=$\frac{\nu}{Q_a} = 8000Hz$

δt ~8.3h(KSVZ) ~61.0h(DFSZ)

R&D towards higher freq.

For better sensitivity and faster scan rates:

Lower (noise) temperatures
Higher magnetic field
Larger effective volume
Improved cavity Q factor

$$P_{signal} = \frac{Q\beta}{(1+\beta)^2} g_{a\gamma\gamma}^2 \left(\frac{\rho_a}{m_a}\right) B_0^2 V C_{010}$$

$$\frac{S}{N} = \frac{P_{signal}}{k_B T_s} \sqrt{\frac{\delta t}{\delta \nu_a}}$$

$$\frac{df}{dt} = \left(\frac{s}{N}\right)^{-2} \frac{Q_a}{Q_L} \left(\frac{P_{signal}}{k_B T_s}\right)^2$$

Future goals: (b) GUT/String inspired axion (& alikes)

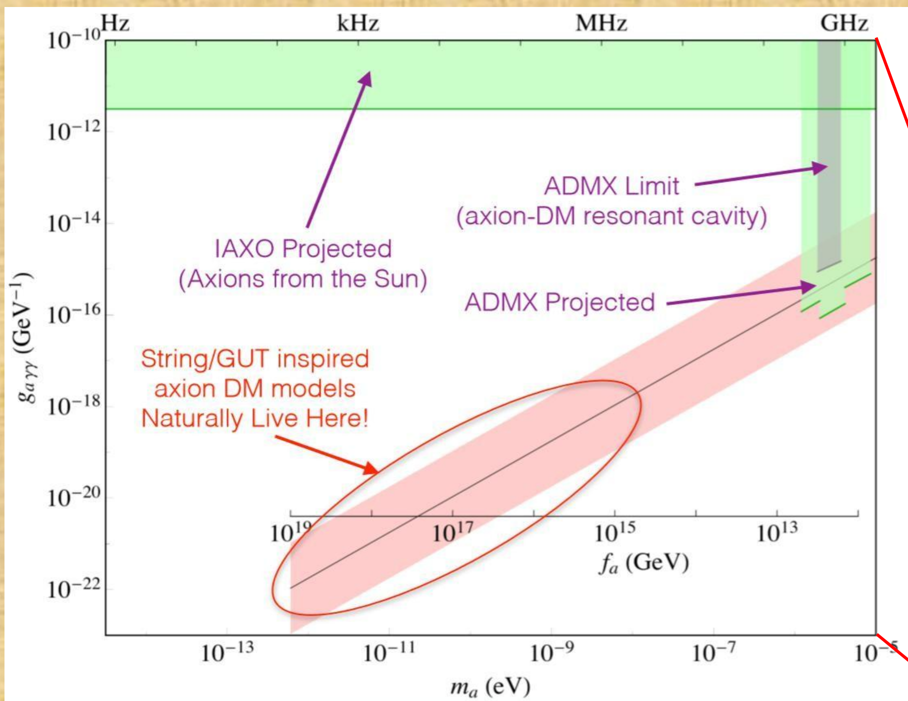

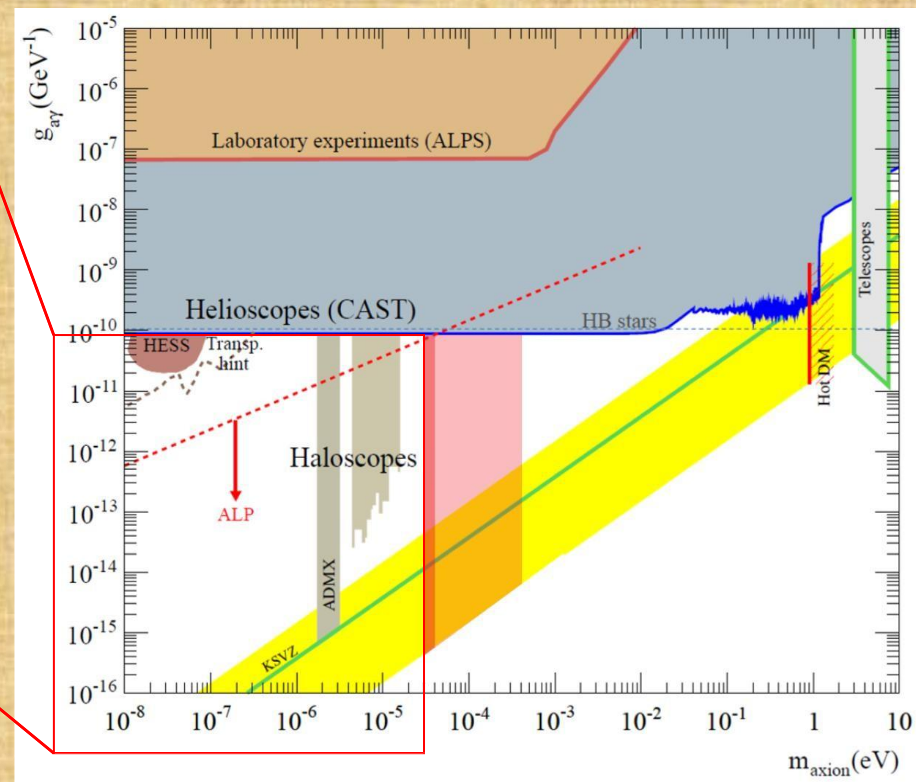

Quantum interferometry and axion haloscope

based on arxiv 2201.08291

with Yu Gao & Zhihui Peng

The quantum properties of the Cavity

Modern cryogenic technology can sustain ~20mK or lower temperature

$$n(\omega_a, T) = \frac{1}{e^{\omega_a / k_B T} - 1}$$

The thermal photon has a very low occupation number n<<1 .

Thus it is useful to consider the quantum picture.

The quantum properties of the Cavity

Modern cryogenic technology can sustain ~20mK or lower temperature

$$n(\omega_a, T) = \frac{1}{e^{\omega_a / k_B T} - 1}$$

The thermal photon has a very low occupation number n<<1 .

Thus it is useful to consider the quantum picture.

The Quantum picture of the Cavity

The axions has a long de-Broglie Wavelength and long coherent time, thus

$$a \approx a_0 \cos(\omega_a t) = \frac{\sqrt{2\rho_a}}{m_a} \cos(\omega_a t)$$

The Quantum picture of the Cavity

The axion photon coupling is

$$\mathcal{L}_{a\gamma\gamma} = -g_{a\gamma\gamma} a \vec{E} \cdot \vec{B}$$

The Quantum picture of the Cavity

The interaction Hamiltonian is

$$
\begin{aligned}
H_I &= -\int d^3x \mathcal{L}_{a\gamma\gamma} \\
&= \left(g_{a\gamma\gamma} \frac{\sqrt{2\rho_a}}{m_a} B_0 \int d^3x \hat{z} \cdot \vec{E} \right) \cos(\omega_a t)
\end{aligned}
$$

The Quantum picture of the Cavity

The electric field operator in the cavity can be expanded

$$\vec{E} = i \sum \sqrt{\frac{\omega_k}{2}} [a_k \vec{U}_k(\vec{r}) e^{-i\omega_k t} - a_k^\dagger \vec{U}_k^*(\vec{r}) e^{i\omega_k t}]$$

where $\vec{U}_k(\vec{r})$ is the cavity modes

The Quantum picture of the Cavity

The transition probability is

$$
\begin{aligned}
P &\approx \left| \langle 1| \int_0^t dt H_I \,|0\rangle \right|^2 \\
&\approx g_{a\gamma\gamma}^2 \frac{\rho_a}{m_a^2} B_0^2 \sum_k \omega_k | \int d^3x \hat{z} \cdot \vec{U}_k^* |^2 \\
&\times \frac{\sin^2[(\omega_k - \omega_a)t/2]}{4[(\omega_k - \omega_a)/2]^2}
\end{aligned}
$$

The Quantum picture of the Cavity

The transition rate is

$$R \approx g_{a\gamma\gamma}^2 \frac{\rho_a}{m_a^2} B_0^2 V \sum_k C_k \omega_k \delta(\omega_k - \omega_a) \approx g_{a\gamma\gamma}^2 \frac{\rho_a}{m_a^2} B_0^2 C_{\omega_a} V Q$$

where

$$C_k = \frac{\left| \int d^3x \, \hat{z} \cdot \vec{U}_k \right|^2}{V \int d^3x |\vec{U}_k|^2}$$

The Quantum picture of the Cavity

The transition rate is enhanced by the cavity quality factor Q even for a single transition.

Typical photon emitting rate of the cavity is order of 10Hz.

The bottleneck of the haloscope

The linear amplifier with a moderate bandwidth adds noise temperature order of T_eff=10K

$$\mathrm{SNR} = \frac{P_{sig}}{k_B T_{eff}} \sqrt{\frac{t}{b}}$$

The quantum interferometry

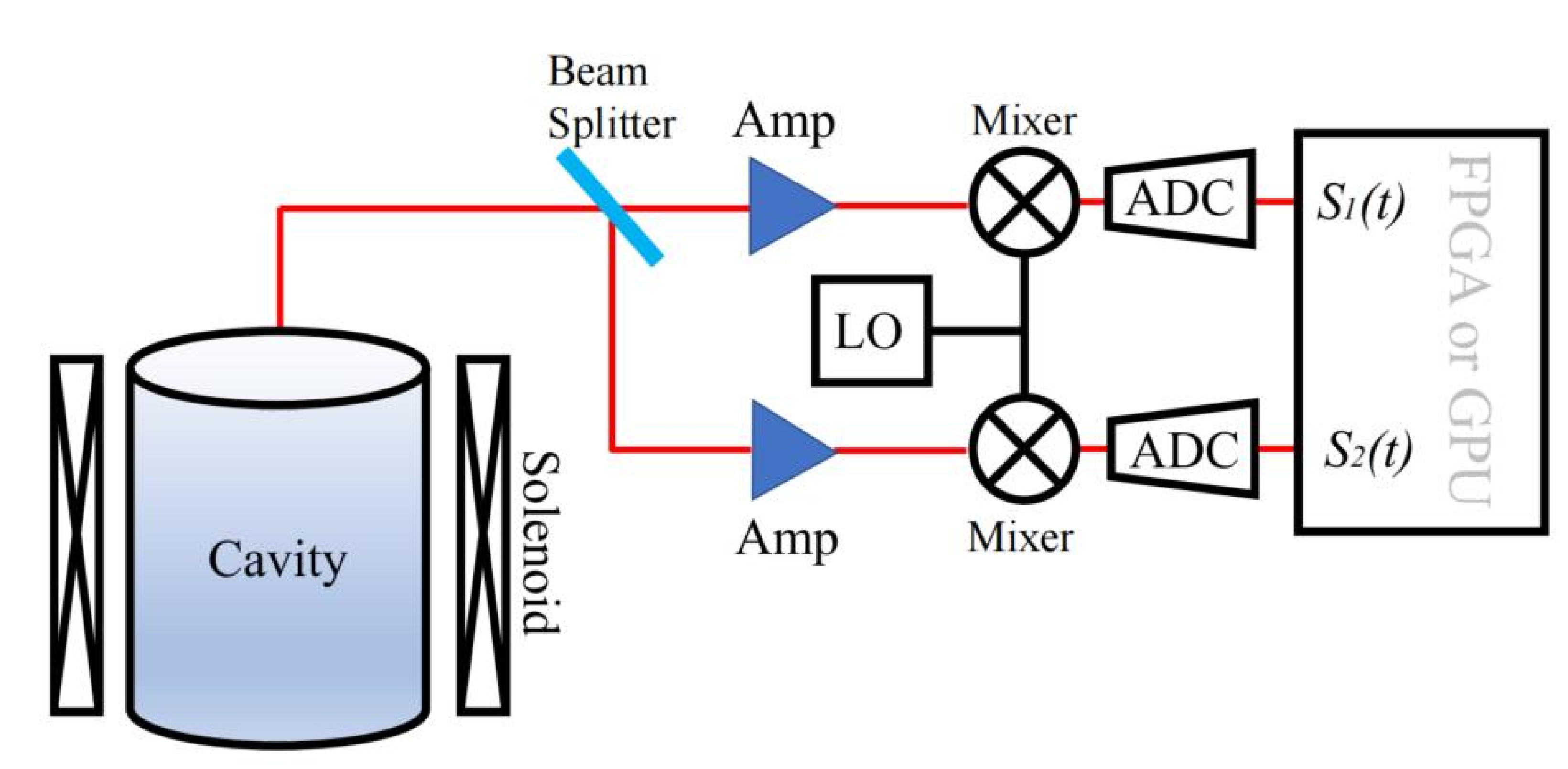

The quantum interferometry (HBT type)

The beam splitter gives two output fields in channel 1 and 2

$$\hat{r}_1 = (\hat{r} + \hat{\nu}_m)/\sqrt{2} \quad \text{and} \quad \hat{r}_2 = (\hat{r} - \hat{\nu}_m)/\sqrt{2}$$

$\hat{r}$ denotes the signal and $\hat{\nu}_m$ denotes the noises.

The quantum interferometry (HBT type)

Then measuring

$$\hat{I}_1 = (\hat{r}_1 + \hat{r}_1^+)/2$$

and

$$\hat{Q}_2 = -i(\hat{r}_2 - \hat{r}_2^+)/2$$

as the real and imaginary part of the field envelopes.

The quantum interferometry (HBT type)

After amplification and mixing, the two path read out is

$$S_i(t) = G_i \hat{r}(t) + \sqrt{G_i^2 - 1} h_i^+(t) + \nu_{m,i}^+(t)$$

The quantum interferometry (HBT type)

The two path instantaneous power function is

$$\langle S_1^*(t)S_2(t)\rangle = G_1G_2\left(\langle \hat{r}^+(t)\hat{r}(t)\rangle + N_{12}\right)$$

where N_{12} is the power of correlated noise in channel 1 and 2

The quantum interferometry (HBT type)

The two path instantaneous power function is

$$\langle S_1^*(t) S_2(t) \rangle = G_1 G_2 \left(\langle \hat{r}^+(t) \hat{r}(t) \rangle + N_{12} \right)$$

the effective temperature of N_{12} is typically 80 mK.

simulated signal

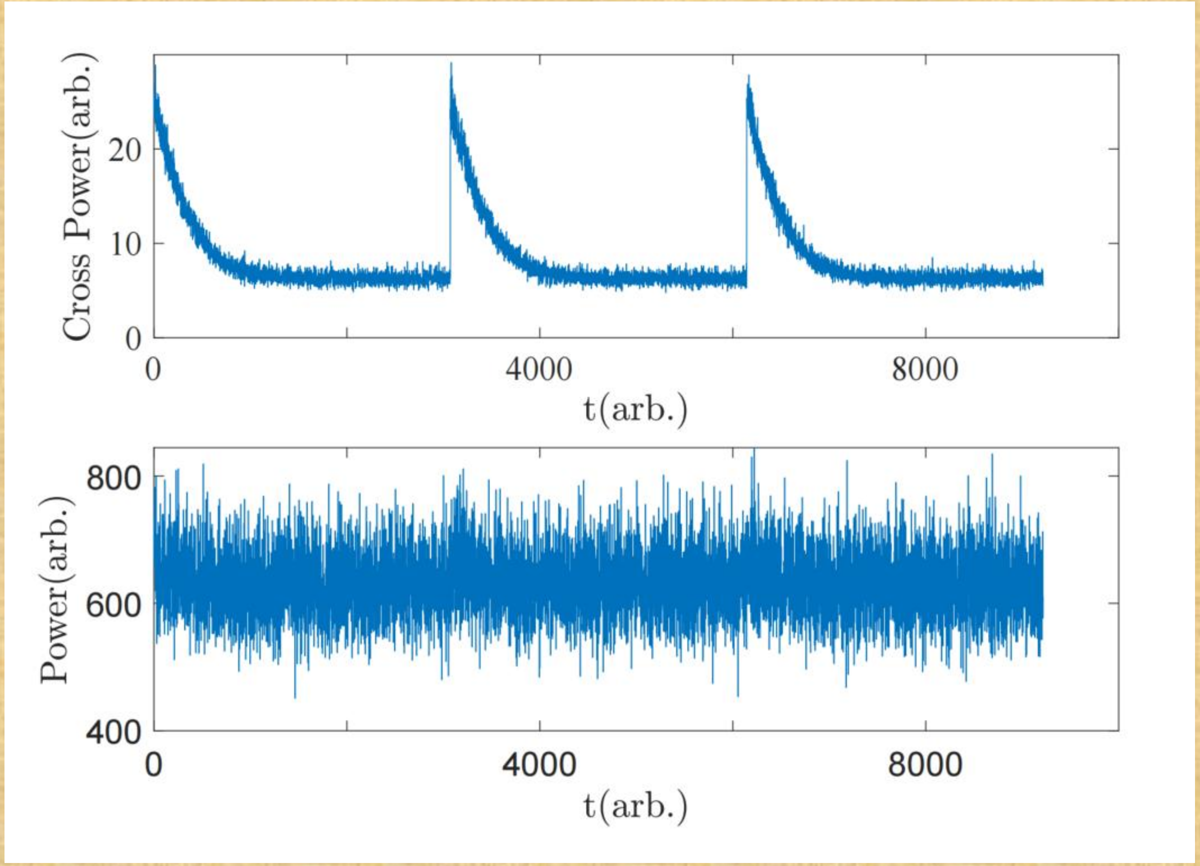

Axions and Inflation

- Cosmological scale correlation length:

  Structures should be Inflated away.

- Structures formed after inflation:

  Correlation length should be much smaller then the horizon

A toy example of axion monodromy:

(4+d)-dimensional gauge field is integrated over a circle in a compact space y:

$$\phi = \int_{S^1} A_1 \qquad\qquad A_1 = \phi(x)\,\eta_1(y)$$

axion is massless if $\Delta\eta_1 = 0$ S^1 is exact periodicity.

Otherwise axion is massive if S^1 is only homologically trivial.

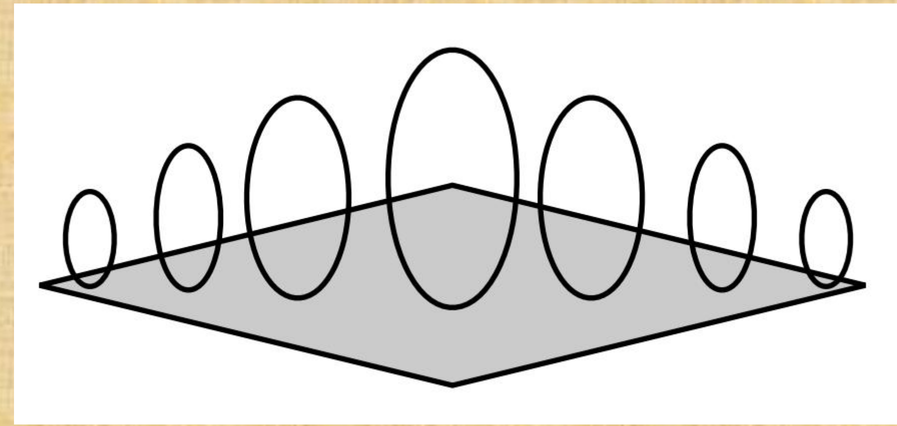

The effective four dimensional potential:

$$V(a) = V_{\text{non-periodic}}(a) + \Lambda^4 \cos\left(\frac{a}{F_a}\right)$$

where the second term is due to string instantons.

$$m_0 = \frac{\Lambda^2}{F_a}, \quad \lambda_0 = -\frac{\Lambda^4}{F_a^4}$$

$$\Lambda^2 \sim M_{Pl}\Lambda_0 e^{-S/2} \qquad \Lambda_0 \sim [10^4\text{GeV}, \quad 10^{18}\text{GeV}]$$

$$V_{\text{non-periodic}}(\phi) = \mu^{4-p}\phi^p$$

Initial fluctuation:

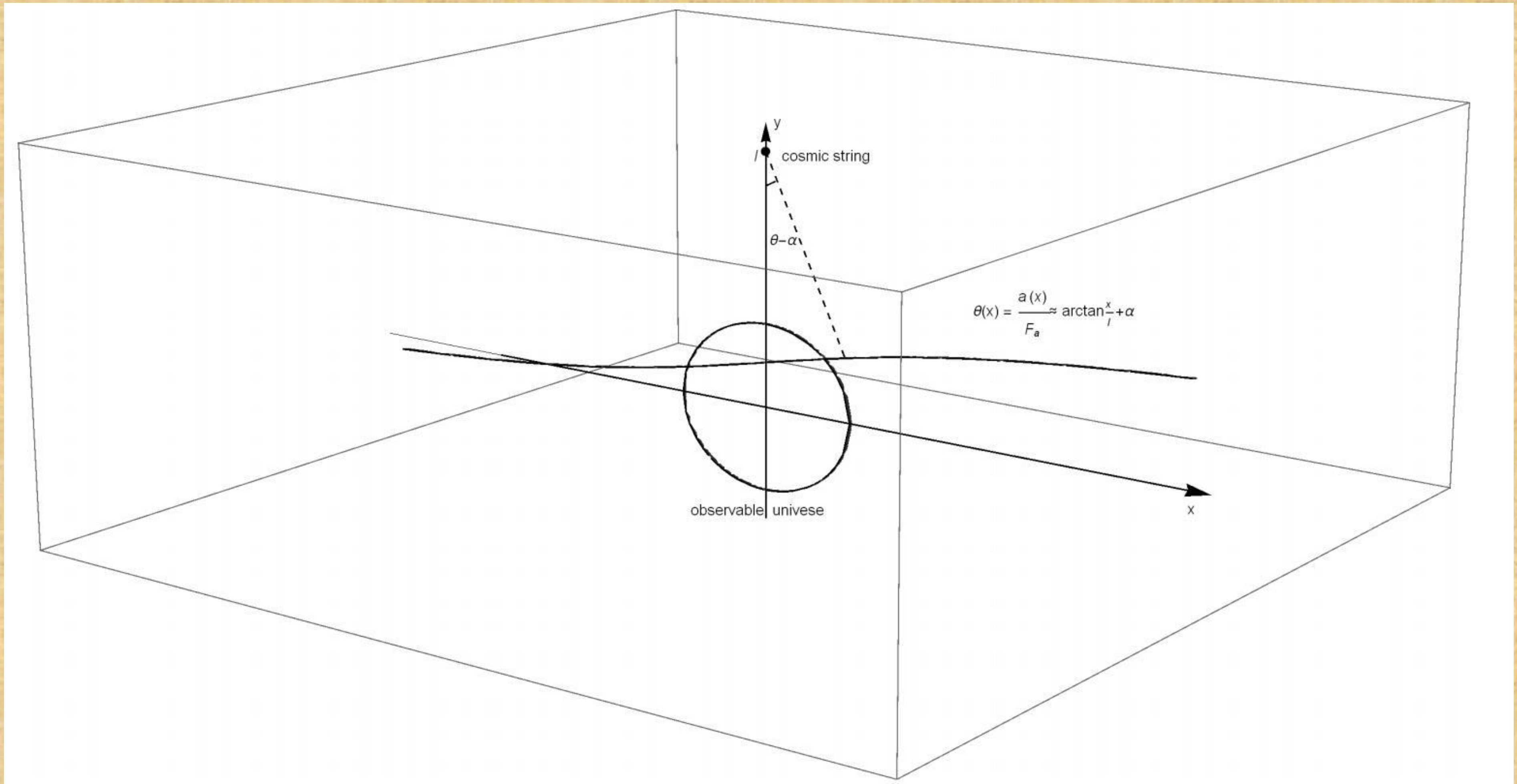

The initial field configuration

- define a parameter *l*

$$\Delta\theta = \theta - \alpha = \frac{a(x)}{F_a} - \alpha = arctan\frac{x}{l-y}$$

- Since *x<<l*, *y<<l*

$$a(\vec{x}) \approx arctan(\frac{x}{l})F_a + \alpha F_a = \bar{a}_0 arctan(\vec{k}\cdot\vec{x}) + \Sigma.$$

$\vec{k} = (1/l, 0, 0)$ defines a preferred direction

$$(\partial_t^2 + 3H\partial_t + \frac{k^2}{R^2})a(\vec{k}, t) = 0$$

- for small k modes, $2\pi(k/R)^{-1} \ll H^{-1}$ protected by topology.

- for large k modes, frozen by causality

$$2\pi(k/R)^{-1} \gg H^{-1} \qquad a(\vec{k}, t) \sim a(\vec{k})$$

The amplitude of fluctuation is scale dependent

- We have a pivot scale: $(1/k') \gtrsim (1/k) =$ *l*

$$arctan(kx) \propto \int (e^{-|k'/k|}/k')e^{-ik'x}dk'$$

- After inflation a domain wall at $\theta = 0$ is outside the observable region.

The energy density ratio

- When *p*=2

$$\rho_a/\rho \propto R$$

- When *p*=4

Remains a constant

Decay of the alps

- When p=2

$$\frac{\rho_a}{\rho} \sim 1.7 \times 10^{-37} \mathrm{GeV}^{-2} \frac{F_a^3}{m}$$

- When p=4

$$\frac{\rho_a}{\rho} \sim \frac{15\bar{a}_0^2}{g_* \pi^2 T_B^4 t_B^2}$$

- For both case the ratio is about 10^{-3}

The hemispherical power asymmetry

$$\Delta T(\hat{n}) = (1 + A\hat{p} \cdot \hat{n})\Delta T_{iso}(\hat{n})$$

- Scale dependent:

A=0.072 for $l_0 < 600$

Amplitude fluctuations due to the quantum effects

$$\rho(\vec{x}) = (1/2)m^2\bar{a}^2(\vec{x})$$

- When the field perturbation is small:

$$\frac{\delta\rho_a(\vec{x})}{\rho_a(\vec{x})} \approx 2\frac{\delta a(\vec{x})}{\bar{a}(\vec{x})} \sim \frac{H_I}{\pi\bar{a}(\vec{x})}$$

The curvature perturbation:

- When the fluctuation spectrum is flat:

$$P_{\Phi,a} \approx (\frac{\rho_a}{\rho})^2(\frac{H_I}{\pi\bar{a}})^2$$

- Therefore :

$$\delta P_{\Phi,a} \; \propto \; 2\delta a\bar{a}$$

The power asymmetry is:

- On large scale:

$$\frac{\Delta P_\Phi}{P_\Phi} = \frac{2\Delta a}{\bar{a}} \frac{P_{\Phi,a}}{P_\Phi} \approx 0.07$$

- Since $\frac{\Delta a}{\bar{a}} = \frac{\bar{a}_0}{\Sigma} arctan(\vec{k} \cdot \vec{x}_{dec})$

  the asymmetry is scale dependent:

$$A(k) \propto \frac{e^{-kl}}{k}$$

The CMB G-Z effect gives a quadrupole coefficient:

- The temperature fluctuation is

$$\frac{\Delta T}{T}(\hat{n}) = 0.066\mu^2\frac{\rho_a}{\rho}(\frac{\bar{a}_0}{\Sigma})^2(\vec{k}\cdot\vec{x}_{de})^2 + ..$$

where

$$\mu = \hat{k}\cdot\hat{n}$$

thus there is a bound $(\frac{\rho_a}{\rho})(\frac{\bar{a}_0}{\Sigma})^2(kx_{de})^2 \lesssim 4.40\times 10^{-4}$

The non-Gaussian bound:

- The Planck mission indicate very small non-Gaussian: $f_{NL} \lesssim 0.01\% \times 10^5$

  and $f_{NL} = (5/4)(\rho/\rho_a)(P_{\Phi,a}/P_{\Phi})^2$

- Therefore : $\frac{1}{8}\left(\frac{P_{\Phi,a}}{P_{\Phi}}\right)^2 \lesssim \frac{\rho_a}{\rho}$

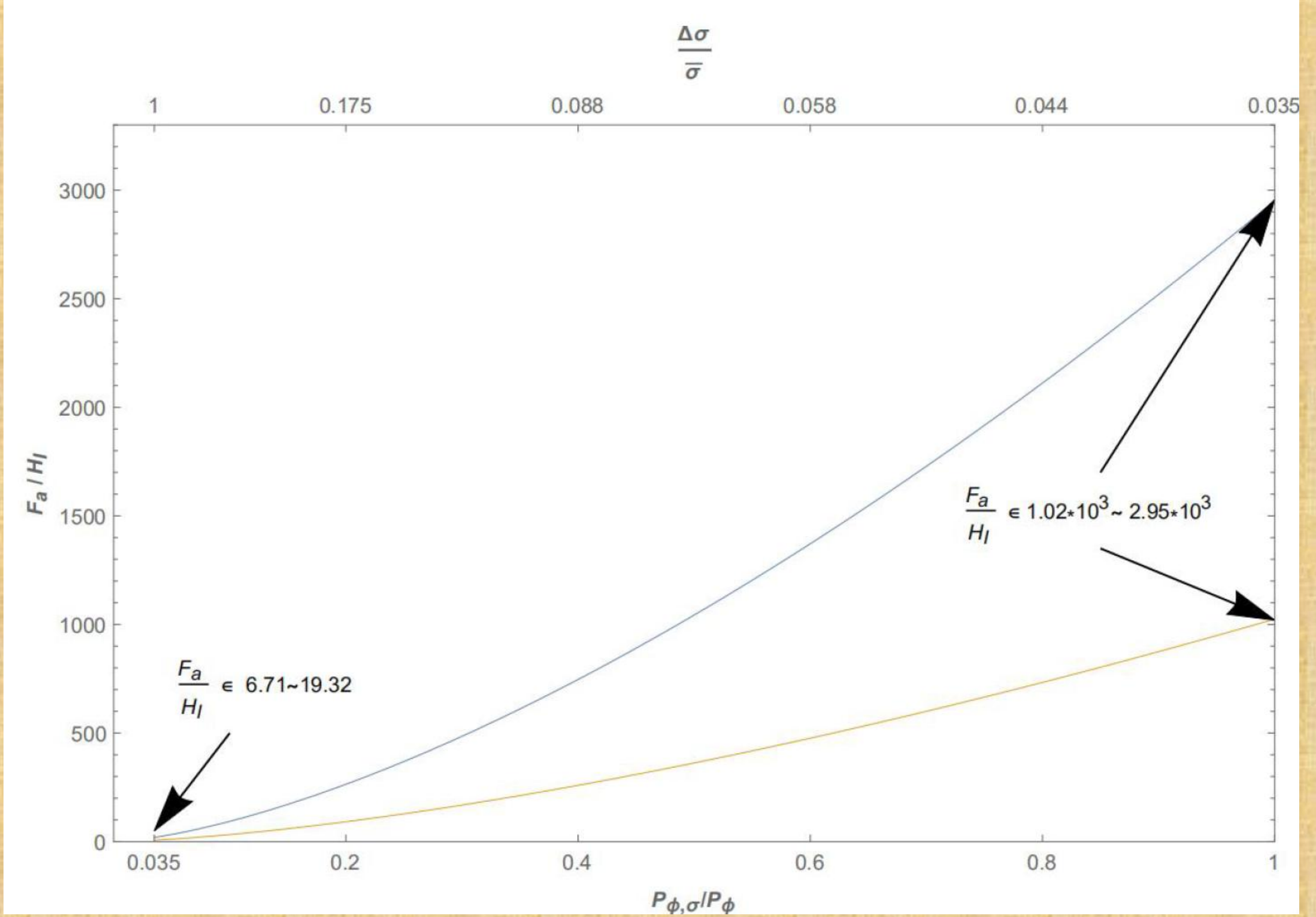

$\frac{\Delta\sigma}{\bar{\sigma}}$
1
0.175
0.088
0.058
0.044
0.035
3000
2500
2000
1500
1000
500
0
F_a / H_l
$\frac{F_a}{H_l} \in 1.02{*}10^3 \sim 2.95{*}10^3$
$\frac{F_a}{H_l} \in 6.71 \sim 19.32$
0.035
0.2
0.4
0.6
0.8
1
$P_{\phi,\sigma}/P_\phi$